Numerical Modeling of Space Plasma Flows: ASTRONUM-2013
ASP Conference Series, Vol. 488
N. V. Pogorelov, E. Audit, and G. P. Zank, eds.

Time-dependent Processes in the Sheath Between the Heliospheric Termination Shock and the Heliopause

N. V. Pogorelov,[1,2] S. N. Borovikov,[2] J. Heerikhuisen,[1,2] T. K. Kim,[1] and G. P. Zank[1,2]

[1]*Department of Space Science, University of Alabama in Huntsville, Huntsville, AL 35805, U.S.A.*

[2]*Center for Space Plasma and Aeronomic Research, University of Alabama in Huntsville, Huntsville, AL 35805, U.S.A.*

Abstract. In this paper, we present the results of our numerical simulation of the solar wind (SW) interaction with the local interstellar medium (LISM). In particular, a solar cycle model based on *Ulysses* measurements allowed us to estimate the interrelationship between heliospheric asymmetries due to the action of the interstellar magnetic field and the decrease in the solar wind ram pressure. We evaluate the possibility to develop an improved approach to derive SW boundary conditions from interplanetary scintillation data. It is shown that solar cycle affects stability of the heliopause in a way favorable for the interpretation of *Voyager 1* "early" penetration into the local interstellar medium. We also show that the heliotail is always a subject of violent Kelvin–Helmholtz instability, which ultimately should make the heliotail indistinguishable from the LISM. Numerical results are obtained with a Multi-Scale Fluid-Kinetic Simulation Suite (MS-FLUKSS), which is a package of numerical codes capable of performing adaptive mesh refinement simulations of complex plasma flows in the presence of discontinuities and charge exchange between ions and neutral atoms. The flow of the ionized component is described with the ideal MHD equations, while the transport of atoms is governed either by the Boltzmann equation or multiple Euler gas dynamics equations. We have enhanced the code with additional physical treatments for the transport of turbulence and acceleration of pickup ions in interplanetary space and at the termination shock.

1. Relationship between geometrical asymmetries and time-dependent processes

Although the heliosphere is the region occupied by the solar wind (SW) plasma, it is common to introduce also the notion of the outer heliosphere as a part of the solar plasma region beyond the solar system whose properties are determined by the SW interaction with the local interstellar medium (LISM). The Sun moves through the LISM, but the SW collides with the LISM for an observer attached to the Sun. Theoretical models of the SW–LISM interaction originate from the seminal paper by Parker (1961), where the SW motion was described hydrodynamically. Numerous heliospheric models have since been developed in attempts to explain experimental data provided by *Prognoz 5* and *6*, *Voyager* 1 and 2 (*V1* and *V2*), *Pioneer 10* and *11*, *ACE*, *Cassini*, *Ulysses*, *EUVE*, *SOHO*, *STEREO*, etc. With *V1* and *V2* crossing the heliospheric termination shock (TS) in December 2004 and August 2007 (Burlaga et al. 2005, 2008; Decker et al. 2005, 2008; Gurnett & Kurth 2005, 2008; Richardson et al. 2008; Stone et al. 2005, 2008) and *V1* entering the LISM in August 2012 (Burlaga et al. 2013; Krimigis et al. 2013; Stone et al. 2013; Webber et al. 2013), understanding the interaction of the SW with the LISM has become one of the most exciting areas of space physics. Understanding the global structure of the outer heliosphere and a number of similar processes in laboratory and astrophysical plasmas requires that we address a variety of physical phenomena. An incomplete list of them includes charge exchange processes between neutral and charged particles, the birth of pick-up ions (PUI), the origin of energetic neutral atoms (ENAs), cosmic ray transport, magnetic field reconnection, particle acceleration, and related turbulence in collisionless plasmas. This requires preferably kinetic modeling of collisions between atoms and ions. On the other hand, pickup ions (PUIs), which are born when the LISM neutral atoms experience charge exchange with SW ions, also require serious attention. The heliospheric interface formed due to the SW–LISM is a unique natural laboratory providing a variety of observational results that require interpretation on a theoretical level.

From a mathematical perspective, we need to solve the 3D MHD equations for the mixture of ions and the kinetic Boltzmann equation to describe the transport of neutral atoms (Izmodenov et al. 2005; Heerikhuisen et al. 2006; Pogorelov et al. 2009b; Heerikhuisen & Pogorelov 2011; Heerikhuisen et al. 2014), interconnected through collisional source terms. Although collisions between ions and atoms are very rare (neutral-neutral collisions are of negligible importance), they are responsible for many physical processes in the heliosphere, such as, SW deceleration, PUI production due to charge exchange, and proton heating due to turbulence generated by instabilities of the PUI distribution function. PUI charge exchange with neutral atoms, on the other hand, creates energetic neutral atoms (ENAs), the fluxes of which is measured by the *Interstellar Boundary Explorer* (*IBEX*), creating all-sky ENA maps (McComas et al. 2009, 2012a,b).

Multi-Scale Fluid-Kinetic Suite (MS-FLUKSS) is a suitable tool to solve rather sophisticated problems related to the SW propagation and its interaction with the LISM (Borovikov et al. 2013; Pogorelov et al. 2010, 2013a). It involves an AMR treatment of ideal MHD flows in the presence of charge exchange between ions and neutrals. Because such collisions are extremely infrequent, we treat the transport of neutral atoms kinetically, by solving the Boltzmann equation with a Monte Carlo method (Heerikhuisen et al. 2006, 2008). As shown in Pogorelov et al. (2009c), a multi-fluid approach (Zank et al. 1996), based on the hydrodynamic treatment of the neutral atom populations born in thermodynamically distinct regions of the heliospheric interface, may be in good agreement the MHD-kinetic simulations. This approach has also been implemented in MS-FLUKSS on both Cartesian and spherical grids.

Recent *Voyager* 1 ($V1$) observations of the nearly vanishing and even negative radial velocity component may have serious consequences for the overall pattern of the SW and LISM plasma flows in the vicinity of the heliopause (HP) and coupling of the interstellar and heliospheric magnetic fields (ISMF and HMF). On the other hand, its penetration into the LISM at about 122 AU raises questions about the time dependence of the inner heliosheath (IHS, a region of the SW plasma between the TS and the HP) width in numerical models. E.g., the heliosheath widths in the steady-state, MHD-kinetic simulations by Pogorelov et al. (2008, 2009b) are 65 AU (in the $V1$ direction) and 48 AU (in the $V2$ direction), and 60 AU ($V1$) and 42 AU ($V2$), respectively for the

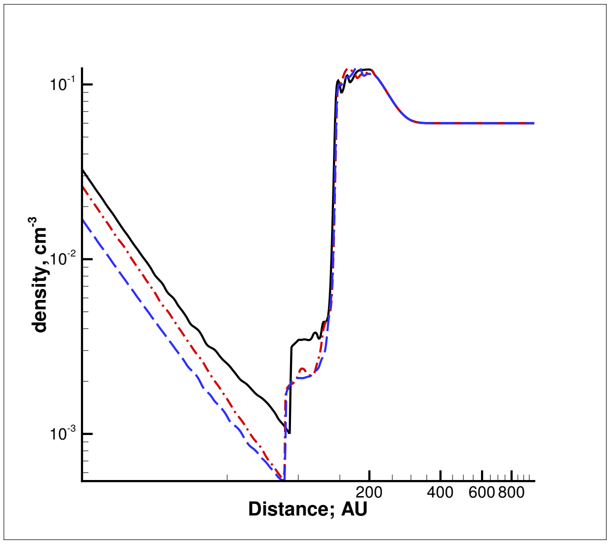

Figure 1. The distributions of plasma density in the direction of the *Voyager 1* trajectory in the solution from Pogorelov et al. (2013b) on the dates of 2002.04 (black solid line), 2006.18 (red dash-dotted line), and 2008.56 (blue long-dashed line).

ISMF strengths $B_\infty = 3\ \mu$G and 4 μG. These numbers clearly contradict observations and unsteady models should be involved.

The asymmetry in the TS heliocentric distances in the directions of *V1* and *V2* spacecraft can be attributed both to the action of the ISMF (Opher et al. 2006; Pogorelov et al. 2006, 2008, 2009b; Ratkiewicz & Grygorczuk 2008) and to time-dependent phenomena (Pogorelov et al. 2013a) in the time interval between the spacecraft crossings of the TS. Charge exchange tends to diminish the asymmetry caused by the ISMF pressure (Pogorelov et al. 2007). On the other hand, increasing the ISMF strength while keeping the neutral H density in the unperturbed LISM constant will usually produce the required TS asymmetry (Pogorelov et al. 2009b). It is therefore necessary to take into account the combined effect of the ISMF and time-dependent phenomena. A simplified solar cycle model developed by Pogorelov et al. (2009a) shows that variations in the HP heliocentric distance are very minor. However, it is known that the ram pressure of the SW was decreasing between *V1* and *V2* crossing the TS. It is therefore interesting to see how the HP heliocentric distance behaves in a more sophisticated solar cycle model based on *Ulysses* observations (Pogorelov et al. 2013b). This model takes into account temporal variations is the SW ram pressure in a 3D fashion. Figure 1 shows the density distributions in the V1 direction at the years of 2002.04 (black solid line), 2006.18 (red dash-dotted line), and 2008.56 (blue long-dashed line). It is clearly seen that the HP position is only slightly changing and remains close to 140 AU. On the other hand, the TS position decreased considerably: from 93 AU to 88 AU. Note that the above model reproduces timing of the TS crossings by *V1* and *V2* with remarkable accuracy.

We conclude that some other physical processes should be taken into account in order to explain the HP crossing at 120 AU instead of 140 AU. We shall return to this subject below. In addition, Pogorelov et al. (2013a,b) demonstrated a transition to chaotic plasma behavior in the IHS, which is the result of the heliospheric current sheet (HCS) being compressed due to the flow deceleration, below the spatial resolution distance. This will be shown to be of importance for stability of the HP at its nose.

2. Interplanetary scintillation data as boundary conditions in the solar wind

Since Ulysses mission is over, we need other sources of 3D, time-dependent boundary conditions at some distance from the Sun to model the SW–LISM interaction. One way to derive them is to start simulations from the solar surface using remote observations. The corona and inner heliosphere experience strong perturbations related to flares and mass-ejection transients. Occasionally, when directed toward Earth, these can cause dramatic and sometimes hazardous conditions in the Earth environment. The solar physics program in the Upper Atmospheric Research Section of the Division of Atmospheric Sciences, National Science Foundation supported extensive research efforts to investigate the connections between eruptive events and magnetic phenomena on the Sun and the corresponding SW structures in the IHS. Since the 1970's, many observing tools have become available: sensitive coronagraphs, both ground-based and space-borne; X-ray imaging telescopes; low-frequency radio telescopes; space-borne kilometric wave radio receivers; and interplanetary scintillation (IPS) arrays. Substantial success was achieved in global numerical modeling of the inner heliosphere within the Solar, Heliospheric, and Interplanetary Environment (SHINE) program. To be efficient, modeling efforts should be based on solar observations from different sources, such as, e. g., *Yohkoh*, *Ulysses*, Solar and Heliospheric Observatory (*SOHO*), *STEREO*, and *Wind* spacecraft, as well as ground-based observations from, e.g., EISCAT, the Mauna Loa Solar Observatory, the Wilcox Solar Observatory (WSO), the National Solar Observatory (NSO), and the Nobeyama Solar Radio Observatory. *Hinode* and Solar Dynamic Observatory (SDO) missions are measuring line-of-sight (LOS) and transverse magnetic field vector components with high resolution. This makes it possible to analyze the origin of solar activity and energy transport from the Sun's surface to the corona and further outwards beyond the critical point to distances of the order of 1 AU using MHD simulations (see, e. g., Detman et al. 2011; Intriligator et al. 2012; Linker et al. 1999, 2011; Lionello et al. 2009; Lugaz & Roussev 2011; Manchester et al. 2006; Odstrcil et al. 2008; Odstrcil & Pizzo 2009; Riley et al. 2006, 2011, 2013; Roussev et al. 2003; Usmanov & Goldstein 2006; Usmanov et al. 2011; Wang et al. 2011; Wu et al. 2006, 2009; Feng et al. 2011).

Daily observations of IPS can be used to map the 3D solar wind structure with reasonable accuracy (see `http://stsw1.stelab.nagoya-u.ac.jp/ips_data-e.html`). In particular, the UCSD time-dependent tomography can reproduce the solar wind speed and density at Earth by iteratively fitting a kinematic solar wind model to IPS and near-Earth spacecraft data (Jackson et al. 1998, 2003, 2010, 2013; Jackson & Hick 2004). However, the kinematic model, which is commensurate with the resolutions available from the IPS data and near-Earth *in situ* plasma data, gradually breaks down as the distance from the Sun increases beyond the orbit of Earth, and a more sophisticated, physics-based model such as a MHD model would be necessary to extrapolate the kinematic solution to the outer heliosphere. Therefore, we performed a 3D MHD simulation using boundary conditions provided by the time-dependent tomography and compared the MHD solution extracted at various locations in the inner heliosphere with spacecraft data and also with the kinematic solution (Kim et al. 2013, 2014). The comparisons show significant differences in proton radial velocity and num-

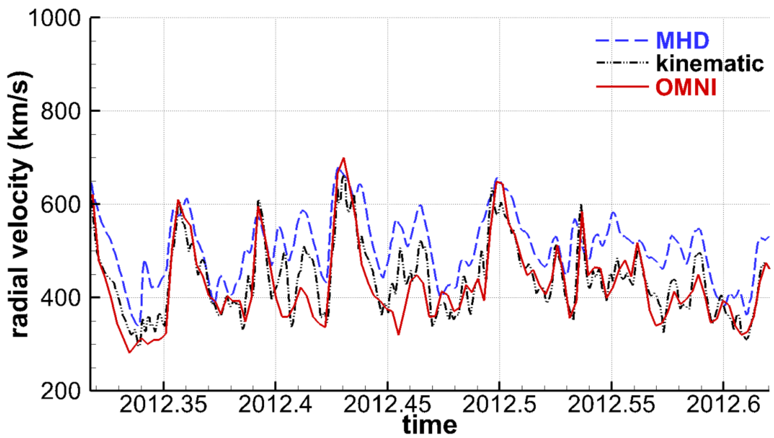

Figure 2. Plasma radial velocity component distributions obtained for a period during the year of 2012: OMNI data (red solid line), kinematic MHD tomography (black dash-dotted line), and MHD simulation with the same inner boundary conditions (blue dashed line).

ber density at Earth and other locations between the MHD solution and both the *in situ* data and the kinematic solution. As shown in Fig.2, the MHD radial velocities are generally greater than the measured values by as much as 150 km/s. Though not shown in the figure, the proton density fluctuations are also markedly larger in the MHD solution. In principle, simple *ad hoc* modifications of the inner boundary conditions can improve the MHD solution at Earth (Kim et al. 2014). However, this is not exactly what we want from observational data. We also came to the conclusion that the inner boundary conditions given by the kinematic model are unlikely to produce MHD results that match IPS and *in situ* data as well as the kinematic model does unless the MHD model is iteratively fit to observational data itself. In the latter case, we will no longer need to perform any additional simulations because the converged result of an MHD-IPS will give us an MHD solution satisfying IPS observations.

3. Magnetic field on the inner side of the heliopause

For the purpose of the following consideration, it is interesting to look at the evolution of the magnetic field strength over a solar cycle. The tilt of the Sun's magnetic axis to its rotation axis changes considerably from a few degrees at solar minima to almost 90° during solar maxima (see, e.g., Fig. 5 in Pogorelov et al. 2013b, produced from the Wilcox Solar Observatory data). This means that the the region containing the global heliospheric current sheet (HCS) will either be very narrow or occupy the whole computational region. However, there always seems to be a region near the HP in the *V1* direction were the HCS should be observed. It is only the width of this region that changes in time (see Fig. 3).

This figure is shown for illustrative purposes only. This region can have more complicated time-dependent structure, as seen, e.g., from Pogorelov et al. (2013b). Of importance is the plasma speed in the direction normal to the HP. If it is small,

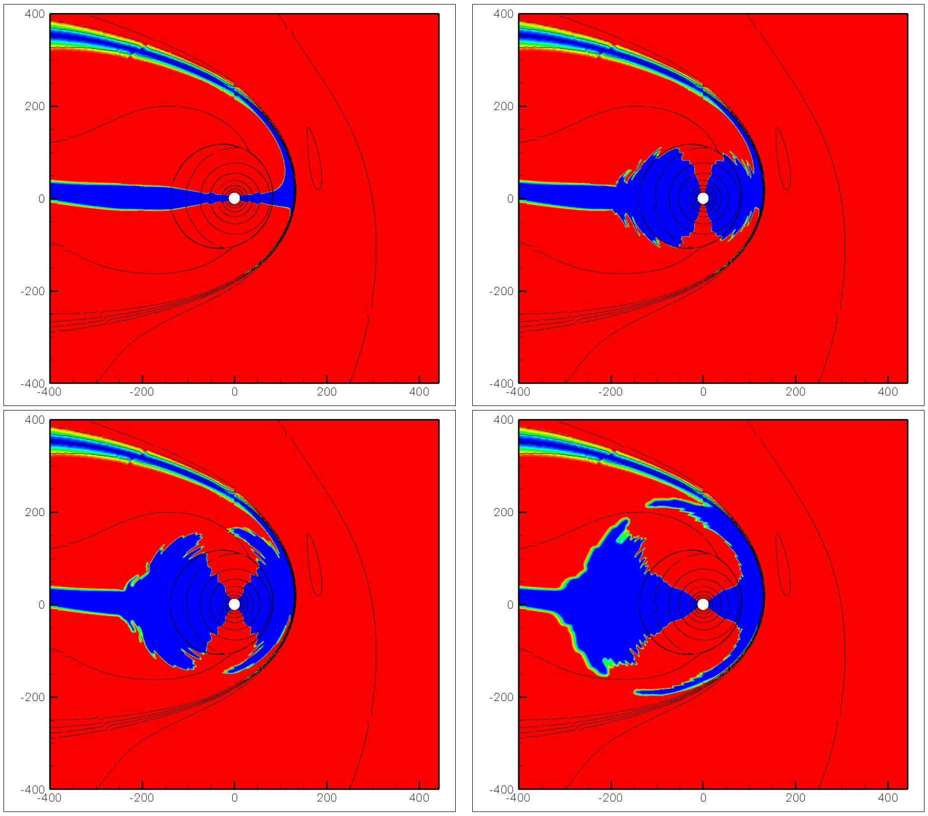

Figure 3. The boundary of the region covered by the HCS (shown with the blue color) using the boundary conditions from Wilcox Solar Observatory data propagated kinematically outward with the level set method. The background plasma distribution is taken from Borovikov et al. (2011).

unipolar sector width becomes very small and can become smaller that the turbulence injection scale. Lazarian & Opher (2009) and Drake et al. (2010) argue that turbulence can also be produced by magnetic reconnection across the HCS. If this happens, the whole region near the HP can be turbulent with a depressed magnetic field (see, e.g. Pogorelov et al. 2013a,b). This results in additional plasma heating and acceleration. It so happens that magnetic field dissipation near the HP helps destabilize the HP and allow LISM plasma penetration deep inside in the heliosphere, which is favorable for the explanation of the recent *V1* data.

4. Instability of the heliopause

Recent observations from the *V1* spacecraft show that it penetrated into the LISM. This is quite surprising because no realistic, steady-state SW model interaction with the LISM gives the inner heliosheath width as narrow as ∼ 30 AU, or the HP at a distance of 122 AU. This includes such models that assume a strong redistribution of the ion energy to the tails in the pickup ion distribution function. It is possible for the heliosphere to shrink considerably by decreasing the ratio of the SW and LISM ram

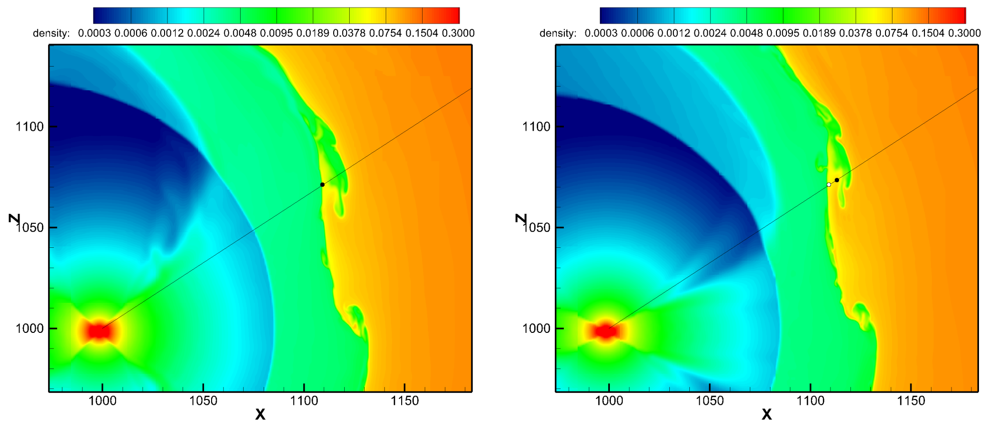

Figure 4. A possible scenario of Voyager 1 moving through the instability. Left panel: initial crossing of the HP. Right panel: position of *V1* two years later as the HP evolves. From Borovikov & Pogorelov (2014) (with permission of the AAS).

pressures. However, our current state of knowledge about the SW and LISM properties (see, e.g., Pogorelov et al. 2013b; Heerikhuisen et al. 2014) tells us that this is very unlikely. Indeed, the SW ram pressure was mostly decreasing over the past decade, but new *IBEX* data show that the LISM ram pressure is likely less than it was expected on the basis of *Ulysses* observation.

Although the HP is likely a mixing layer rather than an ideal MHD discontinuity, its dissipative/resistive width is narrow (Fahr et al. 1986). Instead, it should be subject of different types of instability, which makes mixing of the SW and LISM plasmas "spotty." Borovikov & Pogorelov (2014) showed that the nose of the HP is indeed not a smooth tangential discontinuity, but is Rayleigh–Taylor unstable, which results in the LISM material penetration deep inside the SW. They also showed that the HP flanks are always subject to a Kelvin–Helmholtz (KH) instability.

Ruderman & Fahr (1995) considered the HP nose instability as a shear-flow instability of the KH type. Chalov (1996) investigated the stabilizing effect of the HP curvature. Ruderman & Belov (2010) showed that this instability should rather be classified as a negative-energy instability. Note that the KH instability has been interpreted as due to the interaction of positive and negative canonical energy waves by McKenzie (1970); Cairns (1979); Walker (2000), and Lashmore-Davies (2005). The instabilities are considerably suppressed near the HP nose by the heliospheric magnetic field in steady-state models, but reveal themselves in the presence of solar cycle effects. Arguably, *V1* may be in one of such instability regions and therefore observing plasma densities much higher than those in the pristine SW. These results may be an explanation of the *V1* early penetration into the LISM. Borovikov & Pogorelov (2014) also show that there is a possibility that the spacecraft may start sampling the SW again before it finally leaves the heliosphere as shown in Fig. 4.

Attributed to charge exchange by Liewer et al. (1996) and Zank et al. (1996, 1999), the Rayleigh–Taylor instability of the HP was considered numerically by Florinski et al. (2005) and Borovikov et al. (2008) assuming an axially symmetric configuration of the SW–LISM interaction, which requires the absence of the HMF and the assumption of the LISM velocity and ISMF vectors being parallel to each other. The latter assumption results in the ISMF vanishing at the LISM stagnation point on the HP and ensures a relatively weak ISMF when *V1* crosses the HP. Being a tangential discontinuity, the HP is unconditionally unstable in the absence surface tension (e.g., due to magnetic fields). Magnetic field tension can stabilize the HP in the absence of charge exchange. Charge exchange and magnetic field tension compete with each other. Three-dimensional, steady-state simulations, even performed with an extremely high resolution near the HP ($\sim$ 0.02 AU), showed no signs of instability at the HP nose (Borovikov et al. 2011).

Borovikov & Pogorelov (2014) showed that the solar cycle creates conditions favorable for the HP instability and deep penetration of the LISM plasma into the IHS. The primary reason of the instability is charge exchange, but temporary decreases of the HMF strength at the *V1* latitude prevent the magnetic field tension from stabilizing the HP. As discussed by Fahr et al. (1986) and Ruderman & Fahr (1995), ram pressure variations related to solar cycle may also contribute to the HP destabilization. However, our simulations show violent instabilities in the absence of HMF even for a steady, spherically symmetric SW. Deep penetration of the LISM plasma into the heliosphere is a plausible explanation of *V1* observations.

5. A few words about the heliotail

Jets and collimated outflows are ubiquitous in astrophysics, appearing in environments as different as young stellar objects, accreting and isolated neutron stars, stellar mass black holes, and in supermassive black holes at the centers of Active Galactic Nuclei. Despite the very different length scales, velocities and composition of these various types of jets, they share many basic physical principles. They are typically long, supersonic flows that propagate through and interact with the surrounding medium, exhibiting dynamical behavior on all scales, from the size of the source to the longest scales observed. Charged particles emitted by stars moving through the interstellar space create astrotails which can be very different in shape and length, depending on the astrophysical object under consideration. A notable example is The Guitar Nebula is a spectacular example of an Hα bow shock nebula observed by the Hubble Space Telescope and Chandra (Chatterjee & Cordes 2002). The physics of the interaction is very similar to that of the SW–LISM interaction, but there are substantial differences in the stellar wind confinement topology.

Mira's astrotail observed by the Galaxy Evolution Explorer (Martin et al. 2007) extends to 800,000 AU. Carbon Star IRC+10216, on the contrary, exhibits a very wide astropause and a short heliotail (Sahai & Chronopoulos 2010).

Unfortunately, it is impossible to look at the heliosphere from a distance. Numerical modeling and subsequent comparison with remote observations of the cosmic ray and ENA fluxes may be a good way to explore the heliotail. The first simulation of this kind was performed in an axially symmetric, gas dynamics statement without magnetic field by Izmodenov & Alexashov (2003), who determined that (1) neutral hydrogen atoms qualitatively change the flow pattern of the solar wind and the LISM in the tail region via change exchange, in particular, the heliopause virtually disappear at distances larger than 3,000 AU; (2) at distances above 20,000 AU, the SW becomes indistinguishable from the LISM; (3) the effect of hydrogen atoms makes the SW supersonic starting from 4,000 AU.

We have recently performed numerical simulation of the long heliotail in an MHD-kinetic statement of the problem, where neutral atoms were treated kinetically. This re-

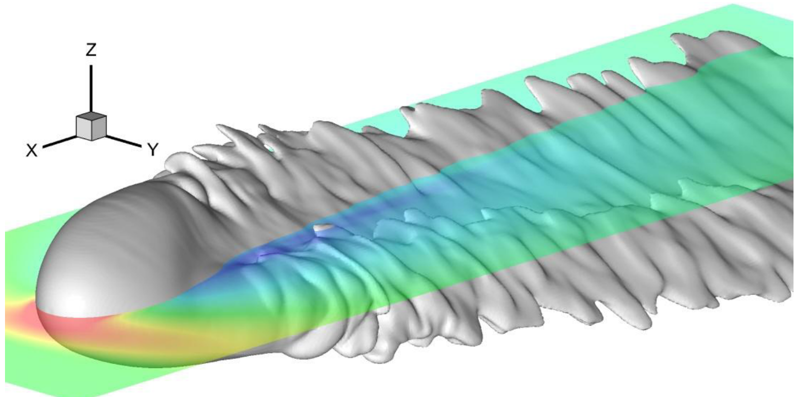

Figure 5. The heliopause identified with a level-set method exhibits strong instability in the tail.

quired substantial modifications to the code in order to make parallel efficiency worthy for such supercomputers as Blue Waters (Borovikov et al. 2013). Although our results are in general agreement with axially-symmetric simulations without magnetic field, there are some differences. Primarily, we found that instability of the HP results in substantial mixing of the the SW and LISM plasmas (see Fig. 5). Our heliotail extends to 5,000 AU and we ensured resolution of at least 5 AU in the tail and heliosheath. The SW plasma becomes fast magnetosonic at 4,200 AU from the Sun. The computational region chosen was 6000 AU cubed. The number of particles in the Monte Carlo simulation of neutral atoms was 1.5×10^{10}. The SW quantities at 1 AU were spherically symmetric: plasma density $n_{\rm p} = 7.4$ cm^{-3}, temperature $T = 51100\,K$, velocity $v = 450$ km/s, and the radial component of magnetic field $B_R = 37.5\ \mu$G. The LISM properties were the same as in McComas et al. (2012a). More detailed results of this research will be published elsewhere.

6. Conclusions

We showed that time-dependent processes are essential for the explanation of spacecraft observations, either made at Earth or in the outer heliosphere, or remotely. This is not only because the SW is generically time-dependent, but also because of the instabilities accompanying the SW–LISM interaction. Of special interest is magnetic reconnection, which remained beyond the scope of this paper. MS-FLUKSS, with its adaptive mesh refinement capabilities, is a powerful tool to address these problems in the future.

Acknowledgments. This work was supported by NASA grants NNX10AE46G, NNX10AC17G, and NNX12AB30G, and Department of Energy grant DE-SC0008334. It was also partially supported by the *IBEX* mission as a part of NASA's Explorer program. We highly appreciate discussions at the team meeting "Heliosheath Processes and Structure of the Heliopause: Modeling Energetic Particles, Cosmic Rays, and Magnetic Fields" supported by the International Space Science Institute in Bern, Switzerland. We acknowledge supercomputer time allocations on Cray XT5 Kraken through NSF XSEDE project MCA07S033. Supercomputer time allocations were also provided on SGI Pleiades by NASA High-End Computing Program award SMD-11-2195 and Blue Waters through NSF PRAC award OCI-1144120.

References

Borovikov, S. N., Heerikhuisen, J., Pogorelov, N. V. 2013, in Astronomical Society of the Pacific Conf. Ser. 474, Numerical Modeling of Space Plasma Flows: ASTRONUM-2012, eds. N. V. Pogorelov, E. Audit, & G. P. Zank, 219–225, San Francisco: ASP

Borovikov, S. N., Pogorelov, N. V., Zank, G. P., Kryukov, I. A. 2008, ApJ, 682, 1404

Borovikov, S. N., Pogorelov, N. V., Burlaga, L. F., Richardson, J. D. 2011, ApJ, 728, L21

Borovikov, S. N., Pogorelov, N. V. 2014, ApJ, 783, L16

Burlaga, L. F., Ness, N. F., Acuña, M. H., Lepping, R. P., Connerney, J. E. P., Stone, E. C., McDonald, F. B. 2005, Science, 309, 2027

Burlaga, L. F., Ness, N. F., Acuña, M. H., Lepping, R. P., Connerney, J. E. P., Richardson, J. D. 2008, Nature, 454, 75

Burlaga, L. F., Ness, N. F., Stone, E. C. 2013, Science, 341, 147

Cairns, R. A. 1979, J. Fluid. Mech., 92, 1

Chalov, S. V. 1996, A&A, 308, 995

Chatterjee, S., Cordes, J.M., ApJ, 575, 407, 2002; ApJ, 600, L51, 2004

Decker, R. B., Krimigis, S. M., Roelof, E. C., Hill, M. E., Armstrong, T. P., Gloeckler, G., Hamilton, D. C., & Lanzerotti, L. J. 2005, Science. 309, 2020

Decker, R. B., Krimigis, S. M., Roelof, E. C., Hill, M. E., Armstrong, T. P., Gloeckler, G., Hamilton, D. C., & Lanzerotti, L. J. 2008, Nature, 454, 67

Detman, T. R., Intriligator, D. S., Dryer, M., Sun, W., Deehr, C. S., Intriligator, J. 2011, J. Geophys. Res., 116, A03105

Drake, J. F., Opher, M., Swisdak, M., Chamoun, J. N. (010, ApJ, 709, 963

Fahr, H. J., Neutsch, W., Grzedzielski, S., Macek, W., Ratkiewicz-Landowska, R. 1986, Space Sci. Rev., 43, 329

Feng, X., Zhang, S., Xiang, C., Yang, L., Jiang, C., Wu, S. T. 2011, ApJ, 734, 50

Florinski, V., Zank, G. P., Pogorelov, N. V. 2005, J. Geophys. Res., 110, A07104

Gurnett, D. A., & Kurt, W. S. 2005, Science, 309, 2025

Gurnett, D. A., & Kurt, W. S. 2008, Nature, 454, 78

Gurnett, D. A., Kurth, W. S., Burlaga, L. F., Ness, N. F. 2013, Science,

Heerikhuisen, J., Florinski, V., Zank, G.P. 2006, J. Geophys. Res., 111(A6), A06110

Heerikhuisen, J., Pogorelov, N. V., Florinski, V., Zank, G. P., & le Roux, J. A. 2008, ApJ, 682, 679

Heerikhuisen, J., & Pogorelov, N.V. (2011), ApJ, 738, 29

Heerikhuisen, J., Zirnstein, E. J., Funsten, H. O., Pogorelov, N. V., Zank, G. P. 2014, ApJ, 784, 73

Intriligator, D. S., Detman, T., Gloecker, G., Gloeckler, C., Dryer, M., Sun, W., Intriligator, J., Deehr, C. 2012, J. Geophys. Res., 117, A06104

Izmodenov, V. V., Alexashov, D. B. 2003, Astronomy Lett., 29, 58

Izmodenov, V., Alexashov, D., & Myasnikov, A. 2005, A&A, 437, L35

Krimigis, S. M., Decker, R. B., Roelof, E. C., et al. 2013, Science, 341, 144

Jackson, B. V., & Hick, P. P. 2004, Astrophys. Space Sci. Library, 314, 355

Jackson, B. V., Hick, P. L., Kojima, M., & Yokobe, A. 1998, J. Geophys. Res., 103, 12049

Jackson, B. V., Hick, P. P., Buffington, A., et al. 2003, Solar Wind Ten, Vol. 679, eds. M. Velli, R. Bruno, and F. Malara (Melville, NY: ASP), 75

Jackson, B. V., Hick, P. P., Bisi, M. M., Clover, J. M., & Buffington, A. 2010, Solar Phys., 265, 245

Jackson, B. V., Clover, J. M., Hick, P. P., et al. 2013, Solar Phys., 285, 151

Kim, T. K., Pogorelov, N. V., Borovikov, S. N., et al. 2013, in Astronomical Society of the Pacific Conf. Proc. 484, eds. Q. Hu & G. P. Zank, 92, San Francisco: ASP